Journal of Engineering Sciences
Vol 13, Issue 05, May /2022
ISSN NO:0377-9254

EFFICIENT ALGORITHM TO CURTAIL THE ATTENUATION IN TERAHERTZ COMMUNICATION NETWORKS

B. NIMISHA[1], D. HEMA VARDHAN REDDY [1], P. KAVERI[1], R. RAKESH BABU[1], Dr. Madhu Babu Sikha[1]

[1]Department of Electronics and Communication Engineering, Malla Reddy Engineering College (A), Secunderabad, Telangana, India

ABSTRACT

Terahertz (THz) communication has been regarded as one promising technology to enhance the transmission capacity of future internet-of-things (IoT) users due to its ultra-wide bandwidth. Nonetheless, one major obstacle that prevents the actual deployment of THz lies in its inherent huge attenuation. Intelligent reflecting surface (IRS) and multiple-input multiple output (MIMO) represent two effective solutions for compensating the large pathloss in THz systems. In this paper, we consideran IRS-aided multi-user THz MIMO system with orthogonal frequency division multiple access, wherethe sparse radio frequency chain antenna structure is adopted for reducing the power consumption. Theobjective is to maximize the weighted sum rate via jointly optimizing the hybrid analog/digital beamforming at the base station and reflection matrix at the IRS. Since the analog beamforming and reflection matrix need to cater all users and subcarriers, it is difficult to directly solve the formulated problem, and thus, an alternatively iterative optimization algorithm is proposed. Specifically, the analog beamforming is designed by solving a MIMO capacity maximization problem, while the digital beamforming and reflection matrix optimization are both tackled using semidefinite relaxation technique. Considering that obtaining perfect channel state information (CSI) is a challenging task in IRS-based systems, we further explore the case with the imperfect CSI for the channels from the IRS to users. Under this setup, we propose a robust beamforming and reflection matrix design scheme for the originally formulated non-convex optimization problem. Finally, simulation results are presented todemonstrate the effectiveness of the proposed algorithms. Index Terms—Hybrid beamforming, Intelligent Reflecting Surfaces, THz, Multiple-input multiple-output.

1. INTRODUCTION

With the rapid proliferation of internet of things (IoTs) users, the future IoT networks need to support the huge transmission capacity [1], [2]. As such, the sub-6 Gigahertz (GHz) and millimeter-wave (mm Wave) may not be able to support these users communications. That beingsaid, terahertz (THz) communication (0.1-10 THz) has been regarded as a promising technology to deal with the above problem due to its ultra-wide bandwidth [3], [4]. However, there are two major shortcomings for THz communications, namely severe signal attenuation and poor diffraction [5]. Multiple-input multiple-output (MIMO) has been recognized as an effective technology to enhance the THz signal strength owing to the high beamforming gain. Indeed, it has been shown that the signal strength grows linearly with the number of antennas at the base station (BS) [6]. Meanwhile, the small wavelength in THz makes it easy to pack more antennas together, and form a massive MIMO array. This way, the problem of severe signal attenuation of THz can be substantially relieved. Nonetheless, the property of poor diffraction still makes THz vulnerable to blocking obstacles that break the line-of-sight (LoS) links. To address this problem,intelligent reflect surface (IRS) can be deployed to create additional links [7], [8], and thus, enhance the performance of THz systems. Being equipped with a large number of

reconfigurablepassive elements [9]– [11], IRS can reflect the incident signals to any direction via adjusting the phase shifts. As a result, when there is no direct link between the transmitter and receiver, communication can still be realized via building a reflective link with the help of the IRS as shown in Fig. 1. Therefore, incorporating MIMO and IRS into the THz communication can effectively enhance the signal reception and reduce the probability of signal blockage. In this paper, we study a multi-user IRS-aided THz MIMO system, where the BS employs sparse RF chain structure for lowering the circuit power consumption [12]. Meanwhile, considering that thewideband THz signals may suffer from frequency selective fading, orthogonal frequency division multiple (OFDM) is also adopted. Based on this system model, we design the hybrid analog/digital beamforming at the BS and the reflection matrix at the IRS for maximizing the weighted sum rate under perfect and imperfect channel state information (CSI). Intelligentreflecting surface (IRS), which enables the reconfiguration of wireless propagation environment by smartly controlling the signal reflections via its massive low-cost passive elements, has recently emerged as a promising new technology for significantly improving the wireless communication coverage, throughput, and energy efficiency [1]–[3]. By jointly adjusting the reflected signal amplitude and/or phase shift at each of the IRS elements according to the dynamic wireless channels, the signals reflected by IRS and propagated through other paths can be constructively combined at the intended receiver to enhance the received signal power. Compared to the traditional active relaying/beamforming techniques, IRS possesses much lower hardware cost and energy consumption due to passive reflection and yet operates in full-duplex without the need of costly self-interference cancellation [1]. However, the enormous passive beamforming gain provided by IRS is achieved at the expense of more overhead for channel estimation in practice, due to the additional channels involved between the IRS and its associatedaccess point (AP)/users. Prior works on IRS mainly focus on the design of reflection coefficients under the assumption of perfect channel state information (CSI) [4], which facilitates in deriving the system performance upper bound but is difficult to realize in practice. In contrast, there has been very limited work on the joint design of practical channel estimation and reflection

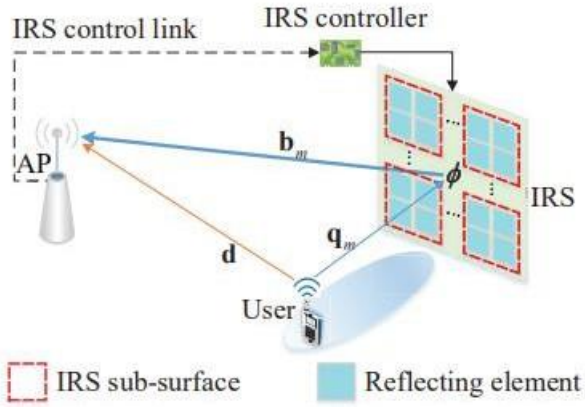

Fig. 1. An illustration of IRS-enhanced OFDM communication in the uplink.optimization under

Vol 13, Issue 05, May /2022
ISSN NO:0377-9254

imperfect CSI tailored to the IRS-aided system, especially for wideband communications. It is worth noting that such design is practically challenging due to the lack of transmitting/receiving as well as signal processing capabilities of the passive IRS elements while their numbers can be practically very large, which thus calls for innovative solutions to tackle these new challenges. As compared to the approach of equipping the IRS with dedicated sensors/receiving circuit to enable its channel estimation, it is more cost-effective to estimate the concatenated user-IRS-AP channels at the AP with properly designed IRS reflection pattern based on the received pilot signals sent by the user and reflected by the IRS [1]. Prior works adopting this method for IRS channel estimation have assumed a simple element-by-element ON/OFF-based reflection pattern [5]–[7], which, however, has two main drawbacks. First, it is practically costly to implement the ON/OFF switching of the massive IRS elements frequently asthis requires separate amplitude control (in addition to phase shift) of each IRS element. Second, the large aperture of IRS is not fully utilized as only a small portion of its elements is switched ON at each time, which degrades the channel estimation accuracy. To overcome the above issues, we propose in this letter a new IRS reflection (phase-shift) pattern for channel estimation by considering the full reflection of the IRS at all time, i.e., all of its elements are switched ON with maximum reflection amplitude during both the channel estimation and data transmission phases. As shown in Fig. 1, we consider a practical wideband IRS enhanced orthogonal frequency division multiplexing (OFDM) system under frequency-selective fading channels, for which a practical transmission protocol is proposed to execute channel estimation and reflection optimization successively. Specifically, a novel phase-shift pattern satisfying the unit-modulus constraint is designed for the IRS to facilitate the concatenated user-IRS-AP channel estimation at the AP based on the uplink pilot signals from the user. A closed-form expression on the channel estimation error is also derived to show the impactof different system parameters. Based on the estimated CSI, the reflection coefficients are then optimized to maximize the strongest time-domain path channel gain, which is shown to have a much lower computational complexity as compared to the semidefinite relaxation (SDR) method in [7] and yet achieve very close performance to it. Notation: Superscripts $(\cdot)^T$, $(\cdot)^H$, and $(\cdot)^{-1}$ stand for transpose, Hermitian transpose, and matrix inversion operations, respectively. $b\cdot c$ is the floor function,denotes the Hadamard product, and rank $(\cdot)$ denotes the matrix rank, and $\angle(\cdot)$ denotes the phase of a complexnumber.

2. LITERATURE SURVREY

The MIMO THz communication has become a research hotspot in recent years. Considering the large signal attenuation, Lin et al. study the indoor short range MIMO THz communications [13], [14]. The authors propose a hybrid analog/digital beamforming to maximize the energy efficiency of the system. Busari et al. consider three hybrid beamforming array structures, namely fully-connected, subconnected and overlapped subarray [15]. Then, a single-path THz channel model is used to investigate the performance of the system under different array structures. Additionally, due to the ultra-wide bandwidth, frequency selective hybrid beamforming design in THz system is necessary. For example, Tan and Dai first analyze the array gain loss in the wideband THz system and then

propose a time delay network to obtain the near-optimal array gain [16]. However, the complexity of the considered system is prohibitively high. Yuan et al. build a 3-D wideband THz channel model and propose a two-stage hybrid analog/digital beamforming for maximizing the capacity of the system [17]. After that, the imperfect CSI is also considered and a robust beamforming design scheme is developed. In parallel, IRS has attracted great attention in the past two years owning to its ability to enable cost-effective and energy efficient communications. Wu and Zhang provide a basic IRS communication system model in [9], based upon which the joint active beamforming at the BS and passive beamforming at the IRS is designed to minimize the system power consumption. In addition, Ning et al. propose to apply THz to IRS [18], and consider the beam training andhybrid analog/digital beamforming. They propose two effective hierarchical codebooks and beamforming design schemes to obtain the near-optimal performance. To study the performance of IRS in frequency selective fading channels, Zhang et al. consider a MIMO OFDM system [19], where only one common set of IRS reflective matrix is designed for all subcarriers. Based on this, a new alternative optimization algorithm is proposed. Yang et al. investigate the channel estimation and beamforming design problem in the IRS-based OFDM system [20], and propose apractical transmission protocol as well as channel estimation scheme. On this basis, a strategy of jointly optimizing power allocation and the reflection matrix is developed for maximizing the achievable rate. Although THz and IRS techniques have been investigated in the literature, e.g., in [9], [13]–[21], most of them do not consider the hybrid beamforming at the BS for IRS communication [9], [18]–[21]. In fact, in a THz-based IRS communication system, the BS should employ a sparse RF antenna structure for reducing the power consumption and the multiple subcarriers transmission technology for overcoming the frequency selection channel fading. As a result, how to design the hybrid analog/digital beamforming at the BS and reflectionmatrix at the IRS catering to all subchannels will be challenging. In addition, how to obtain the perfect CSI remains a non-trivial task for IRS-based reflection links. For the direct link from the BS to users, the CSI can be readily estimated by conventional channel estimation methods. For the indirect link from the BS to the IRS, the CSI is also relatively easy to obtain since the locations of IRS and BS are fixed. However, the accurate CSIs of reflection links from the IRS tousers are usually difficult to obtain due to the mobility of users. Nonetheless, [9], [18]–[21] all assume perfect CSI. Although Zhou et al. investigate the robust beamforming design in an IRS system [22], the conventional multiple antenna structure and single carrier scenario are considered.

3. PROPOSED METHOD

We consider an IRS-aided THz multi-user MIMO system with OFDMA as shown in Fig. 1, where the BS is equipped with NTX antennas and NRF (NRF ≤ NTX) RF chains. The diagram of the sparse RF chain at the BS is illustrated in Fig. 2. We assume that there are no direct links between BS and users due to the blockage of walls or other obstacles, and the users can only receive the reflected signals from IRS. Let NIRS, M and K denote the number of IRS elements, users and subcarriers, respectively. We assume that the CSIs of all links can be obtained using existing channel estimation schemes proposed in broadband IRS system [23]–[25]. In addition, the computation of resource allocation is executed in BS, and then the BS needs to convey the resource allocation results (refection matrix of the IRS) to IRS. As shown in Fig. 1, the IRS phased shifts are controlled by an attached controller. Therefore, the BS can transmit the reflection matrix to controller via a dedicated separate wireless

control link [9]. The received signal on the kth subcarrier at the mth user can be expressed as

$$y_m[k] = \mathbf{G}_m[k]\mathbf{F}\mathbf{v}_m[k]x_m[k] + \sum_{j\neq m}^{M} \mathbf{G}_m[k]\mathbf{F}\mathbf{v}_j[k]x_j[k] + n_m[k]$$

$$\mathbf{G}_m[k] = G_t G_r \eta_k \widehat{\mathbf{g}}_m[k]\boldsymbol{\Phi}\widehat{\mathbf{H}}[k]$$

with Gt and Gr as the transmit and receive antenna gains, respectively, and ηk as the pathloss compensation factor [18]. bgm[k] ∈ C 1×NIRS denotes the channel vector from IRS to the mth user on the kth subcarrier, Φ ∈ C NIRS×NIRS is the reflection coefficient matrix with Φ = diag{φ1, ..., φNIRS }, Hb[k] ∈ C NIRS×NTX represents the channel matrix from BS to IRS on the kth subcarrier, F ∈ C NTX×NRF is the analog beamforming matrix with F = [f1, ...,fNRF], vm[k] ∈ C NRF×1 and xm[k] denote the digital beamforming and transmit signal for the mth user on the kth subcarrier, respectively, nm[k] is the independent and identically distributed (i.i.d.) additive white Gaussian noise (AWGN) with zero-mean and variance N0. In (1), the first term is the designed signal, while the second term is the multi-user interference that must be mitigated by designing proper digital beamforming and reflection matrix. Next, we present the
THz channel model. Let fc and B, respectively, represent the central frequency and bandwidth. Then, the frequency band of the kth subcarrier can be expressed as

fk = fc + B K (k − 1 − K−1 2), k = 1, 2, ..., K.

Although there are a few scattering components in THz communication, their power are much lower (more than 20 dB) than that of LoS component [26], and thus, we only consider the LoS component and ignore the other scattering components. Accordingly, the channel matrix Hb[k] can be expressed as

$$\widehat{\mathbf{H}}[k] = q(f_k, d)\mathbf{H}[k],$$

where q(fk, d) is the complex path gain satisfying

$$\mathbf{a}_t(\theta_k) = \frac{1}{\sqrt{N_{\mathrm{TX}}}}\left[1, e^{j\pi\theta_k}, e^{j2\pi\theta_k}, \cdots, e^{j(N_{\mathrm{TX}}-1)\pi\theta_k}\right]^T,$$
$$\mathbf{a}_r(\varphi_k) = \frac{1}{\sqrt{N_{\mathrm{IRS}}}}\left[1, e^{j\pi\varphi_k}, e^{j2\pi\varphi_k}, \cdots, e^{j(N_{\mathrm{IRS}}-1)\pi\varphi_k}\right]^T.$$

Here, θk = 2d0 fk sin(ϕt)/c and φk = 2d0 fk sin(ϕr)/c, d0 denotes the antenna distance, and ϕt/ϕr ∈ [−π/2,

π/2] are, respectively, angle of departure (AoD) and angle of arrival (AoA). Similarly, gm[k] can be expressed as

$$\widehat{\mathbf{g}}_m[k] = q(f_k, d_m)\mathbf{g}_m[k],$$

where $\mathbf{g}_m[k] = \frac{1}{\sqrt{N_{\text{IRS}}}}\left[1, e^{j\pi\varphi_{k,m}}, e^{j2\pi\varphi_{k,m}}, \cdots, e^{j(N_{\text{IRS}}-1)\pi\varphi_{k,m}}\right]$,
$q(f_k, d_m)$ is defined as

$$q(f_k, d_m) = \frac{c}{4\pi f_k d_m} e^{-\frac{1}{2}\tau(f_k)d_m},$$

with dm as the distance from the IRS to the mth user. The BS-IRS-user m link channel can such be expressed as

$$\mathbf{G}_m[k] = u_m[k]\mathbf{g}_m[k]\mathbf{\Phi}\mathbf{H}[k],$$

$$\eta_k q(f_k, d) q(f_k, d_m) = \frac{\chi c}{8\sqrt{\pi^3} f_k d d_m} e^{-\frac{1}{2}\tau(f_k)(d+d_m)},$$

$$y_m[k] = u_m[k]\mathbf{g}_m[k]\mathbf{\Phi}\mathbf{H}[k]\mathbf{F}\mathbf{v}_m[k]x_m[k] + \sum_{j\neq m}^{M} u_m[k]\mathbf{g}_m[k]\mathbf{\Phi}\mathbf{H}[k]\mathbf{F}\mathbf{v}_j[k]x_j[k] + n_m[k].$$

where χ is the IRS element gain. Finally, we rewrite (1) as

we consider an uplink OFDM system, where an IRS is deployed to assist in the transmission from a user (in its vicinity) to an AP, both of which are equipped with a single antenna. Note that the IRS is practically composed of a large number of passive reflecting elements to maximize its reflection power, which, however, incurs high overhead/complexity for channel estimation and reflection optimization. By grouping adjacent elements of the IRS with high channel correlation into a sub-surface to share a common reflection coefficient [7], the complexity of channel estimation and reflection design can be significantly reduced. Accordingly, the IRS composed of K reflecting elements is divided into M sub-surfaces, each of which consists of K^{-} = K/M adjacent elements, e.g., K^{-} = 4 as illustrated in Fig. 1. Moreover, the IRS is connected to a smart controller to enable dynamic adjustment of its elements' individual reflections. In this letter, quasi-static frequency-selective fading channels are considered for both the user→AP direct link and the user→IRS→AP reflecting link, which remain approximately constant within the transmission frame of our interest. This is a valid assumption as IRS is practically used to mainly support low-mobility users in its neighborhood only.with OFDM, the total bandwidth allocated to the user is equally divided into N sub-carriers, which are indexed by n ∈ N , {0, 1, . . . , N − 1}. For simplicity, we assume that the total transmission power at the user Pt is equally allocated over the N sub-carriers with the power at each sub-carrier given by pn = Pt/N, ∀n ∈ N . Without loss of generality, it is assumed that the baseband equivalent

Vol 13, Issue 05, May /2022
ISSN NO:0377-9254

channels of both the direct link and the reflecting link have the maximum delay spread of L taps in the time domain. At the user side, each OFDM symbol x , [X0, X1, . . .

, XN−1] T is first transformed into the time domain via an N-point inverse discrete Fourier transform (IDFT), and then appended by a cyclic prefix (CP) of length Lcp, which is assumed to be longer than the maximum delay spread of all channels, i.e., Lcp ≥ L. At the AP side, after removing the CP and performing the N-point discrete Fourier transform (DFT), the equivalent baseband received signal in the frequency domain is given by

4. EXISTING METHOD

With OFDM, the total bandwidth allocated to the user is equally divided into N sub- carriers, which are indexed by n ∈ N , {0, 1, . . . , N − 1}. For simplicity, we assume that the total transmission power at the user Pt is equally allocated over the N sub-carriers with the power at each sub-carrier given by pn = Pt/N, ∀n ∈ N . Without loss of generality, it is assumed that the baseband equivalent channels of both the direct link and the reflecting link have the maximum delay spread of L taps in the time domain. At the user side, each OFDM symbol x , [X0, X1, . . . , XN−1] T is first transformed into the time domain via an N-point inverse discrete Fourier transform (IDFT), and then appended by a cyclic prefix (CP) of length Lcp, which is assumed to be longer than the maximum delay spread of all channels, i.e., Lcp ≥ L. At the AP side, after removing the CP and performing the N-point discrete Fourier transform (DFT), the equivalent baseband received signal in the frequency domain is given by where y , [Y0, Y1, . . . , YN−1] T is the received OFDM symbol, X = diag (x) is the diagonal matrix of the OFDM symbol x, d , [D0, D1, . . . , DN−1] T ∈ C N×1 is the channel frequency response (CFR) of the user→AP direct link, qm ∈ C N×1 is the aggregated CFR of the user→IRS link associated with the m-th sub-surface, φm denotes the common reflection coefficient within the m-th sub-surface, bm ∈ C N×1 is the aggregated CFR of the IRS→AP link associated with the mth sub-surface, and v , [V0, V1, . . . , VN−1] T ∼ Nc(0, σ2 IN) is the additive white Gaussian noise (AWGN) vector. In addition, the reflection coefficient φm characterizes the equivalent interaction of the m-th sub-surface with the incident signal, which can be expressed as [4]

5. RESULTS

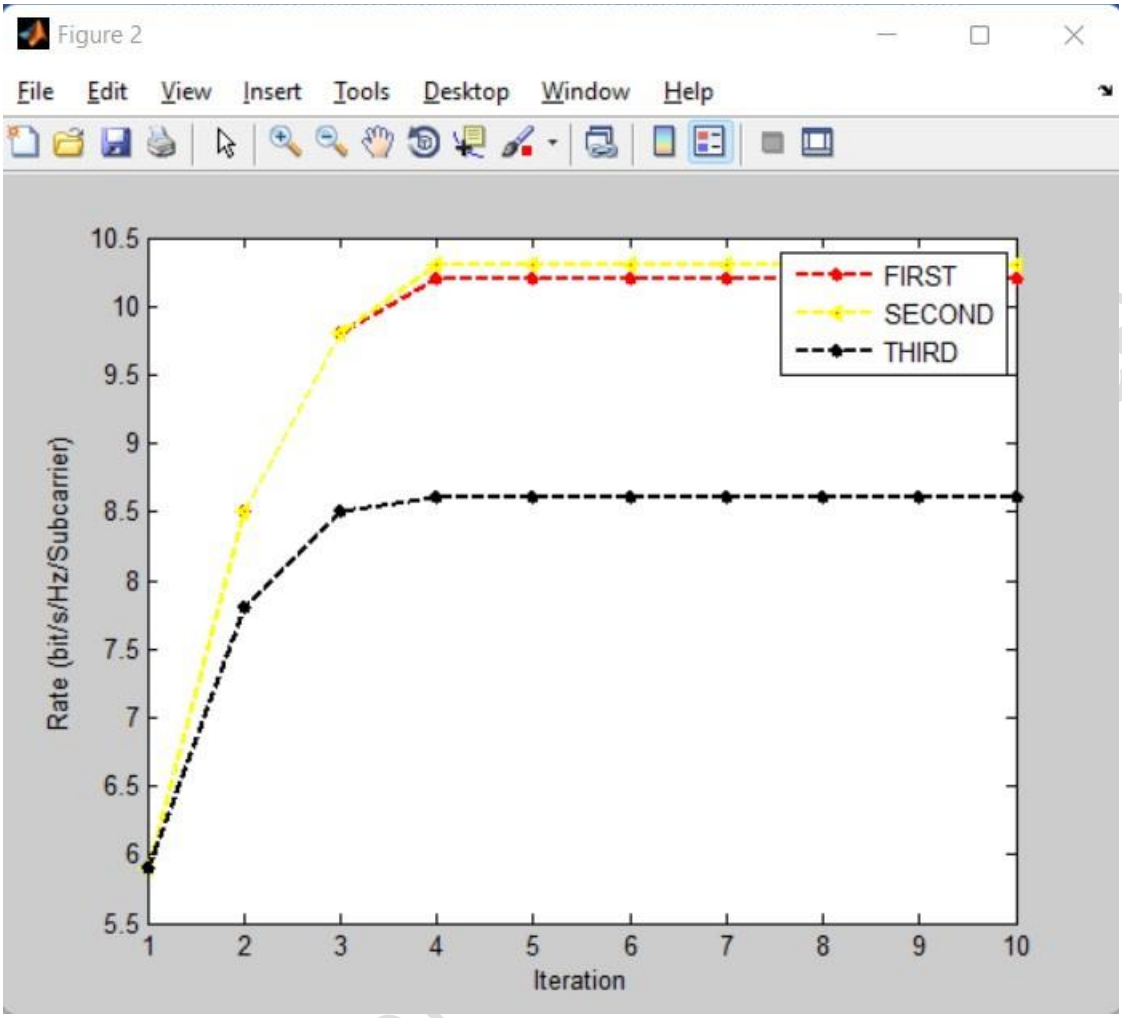

Fig.: The rate versus iteration for solving the reflection matrix.

shows the convergence performance of the proposed inner iterativealgorithm for solving the digital beamforming & refraction matrix.

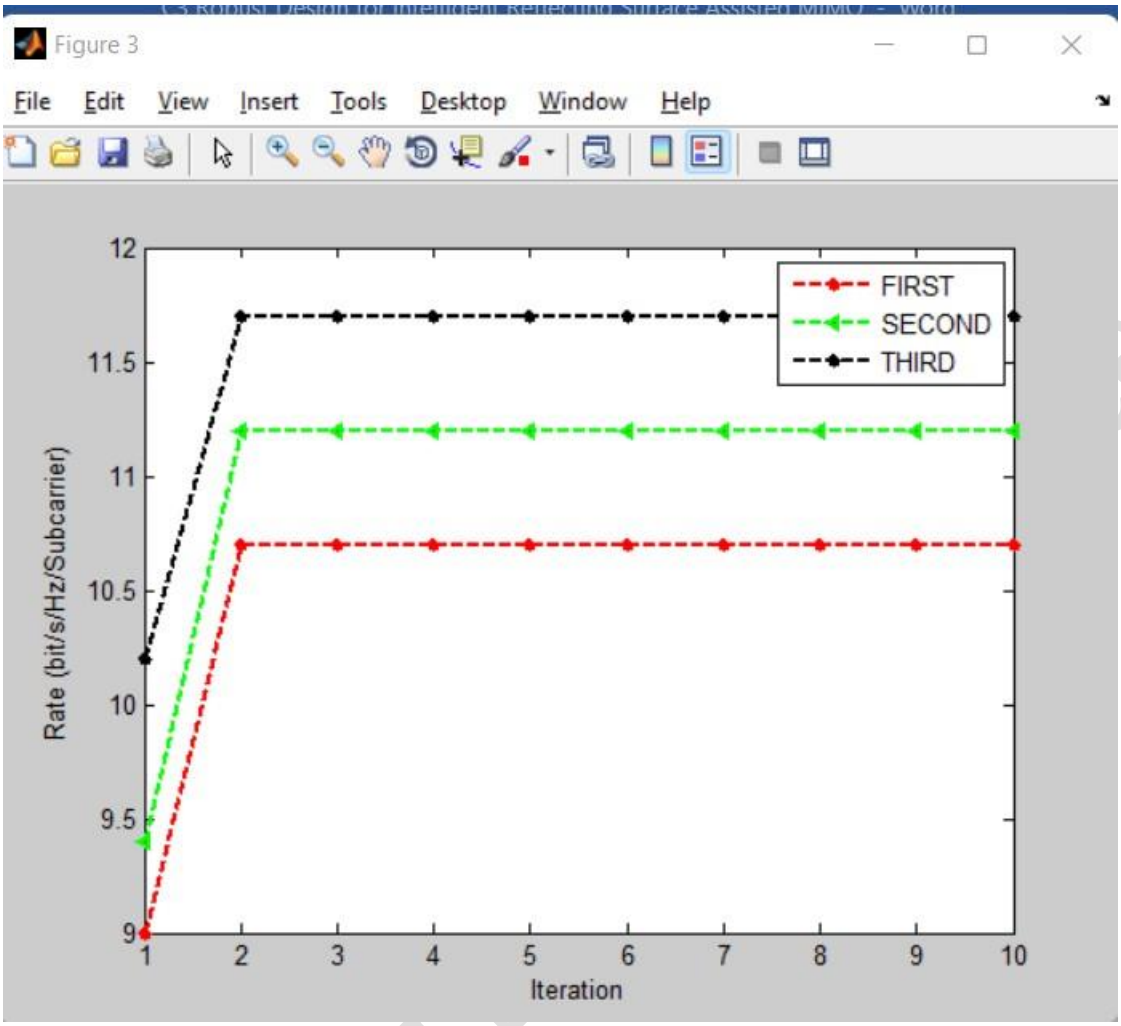

Fig.: The rate versus iteration for the proposed Algorithm 1.

The convergence performance of Algorithm 1 order different estimation errors is plotted in fig.7.6, where we set the maximum transmit power P_{max} *and* $a_{m.}$ It is clear that the rate tends to stabilize after 3 iterations, which demonstrates the fast convergence of the proposed algorithm, $\in=0$ which means perfect CSIS between the IRS and users.

Vol 13, Issue 05, May /2022
ISSN NO:0377-9254

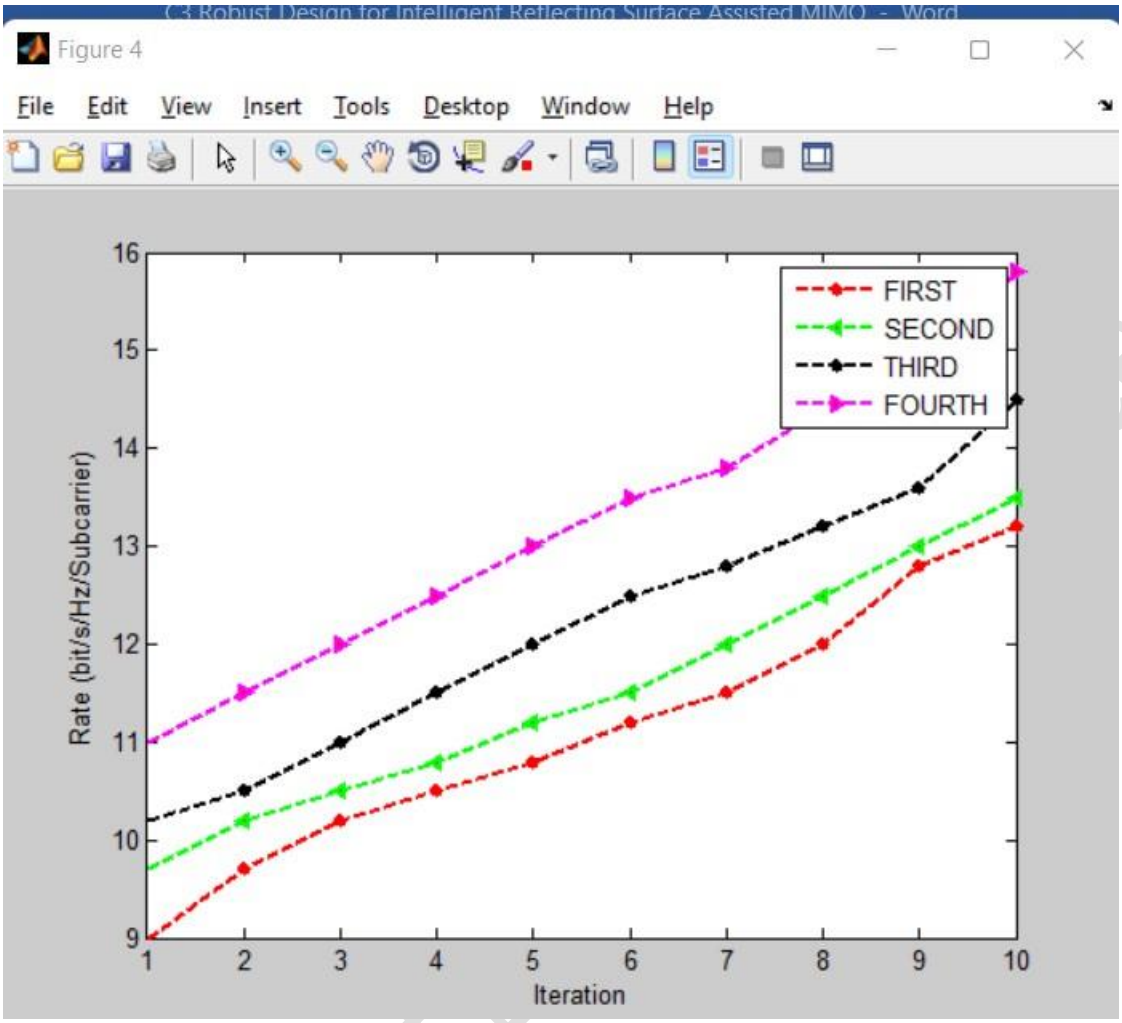

Fig.: The rate versus the allowable maximum transit power.

It shows the rate versus P_{max} under different estimation errors, where we set a_m=1, $w_c$plot the rate under the fussy digital structure, namely each antenna is connected to each RF chain.

It is clear that the rate under the fussy digital structure is higher than that under the space RF chain structure for the same condition, while the circuit power consumption is very high for the former.

This is also one of the reasons for which the sparse RF chain structure is usually adopted when the ultra high frequency carrier is applied.

Journal of Engineering Sciences
Vol 13, Issue 05, May /2022
ISSN NO:0377-9254

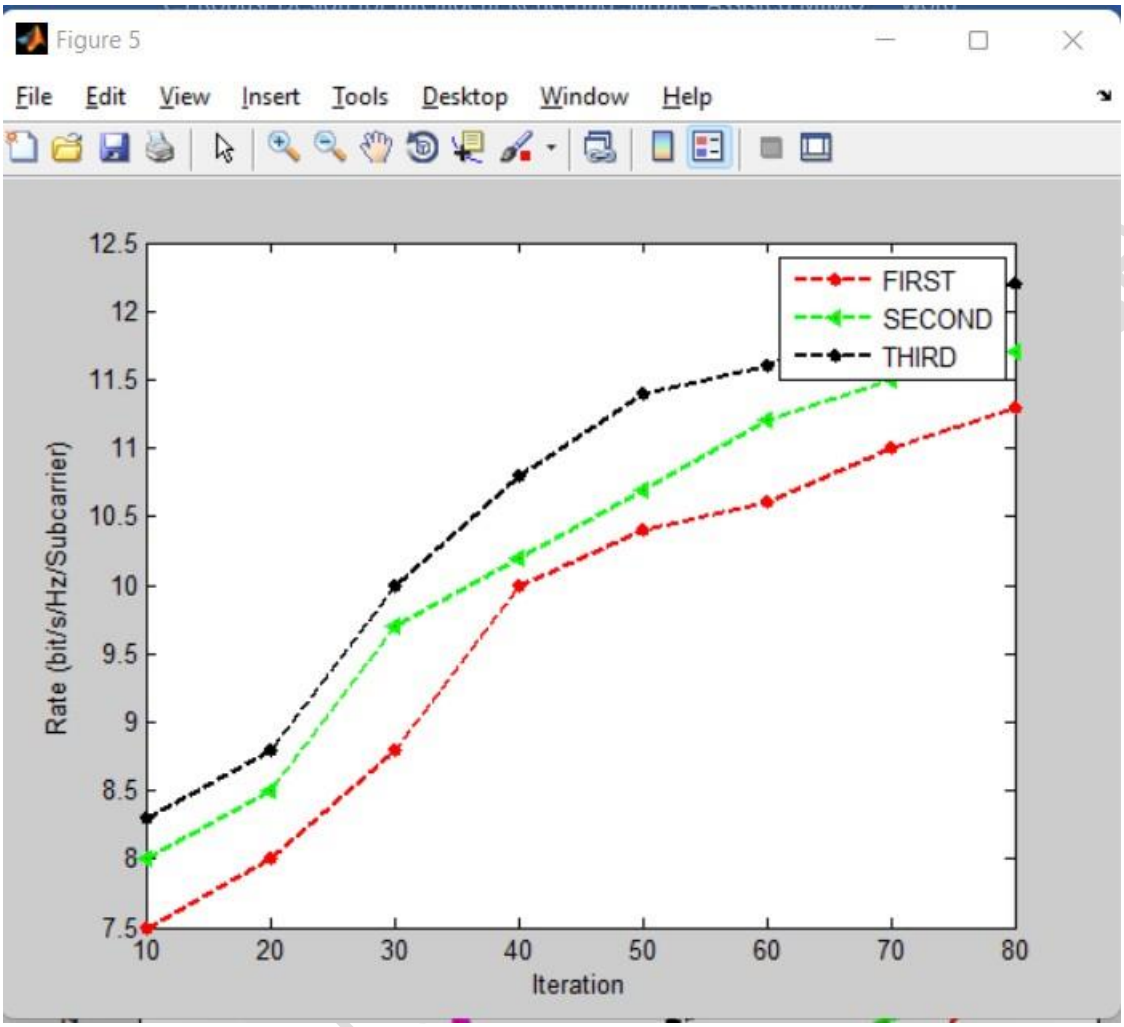

Fig. The rate versus the number of antennas.

In fig.we plot the rate under different antennas where we set P_{max}=4dB and a_m=1. It is obvious that the rate increases with the number of antennas, but with a decreasing slope.

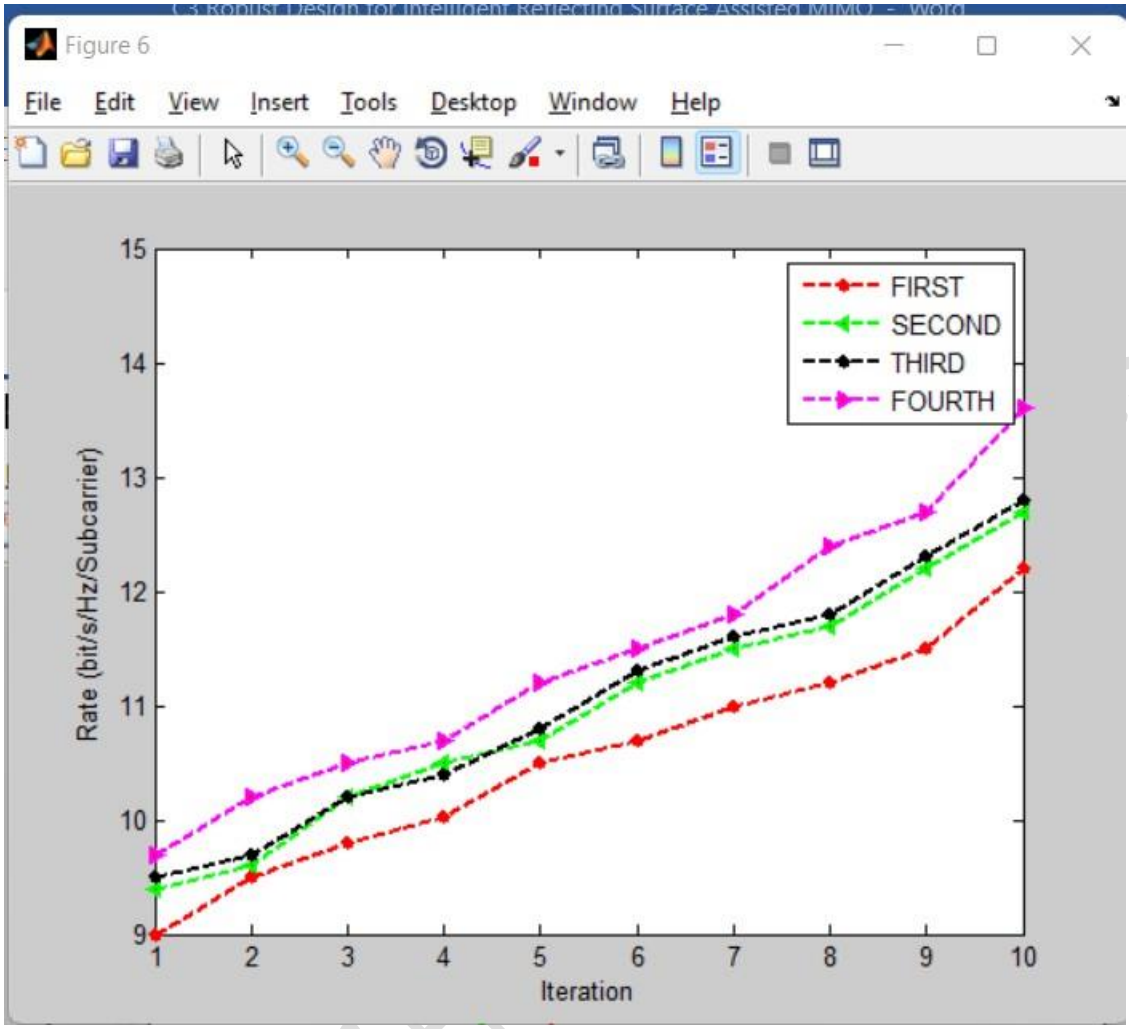

Fig.: The rate versus the allowable maximum transmit power with different weights.

In Fig. we plot the rate versus P_{max} for different number of IRS refraction elements with $\in = 0$. It is observed that a large number of IRS refraction elements leads to a higher rate. This is because a higher beamforming gain can be achieved when there are either more antennas at the BS or more refraction elements at the IRS.

6. CONCLUSION

In this paper, we have considered an IRS-aided THz MIMO-OFDMA system, where the BS is equipped with a sparse RF chain structure. First, we have proposed a joint hybrid analog/digital beamforming and reflection matrix design to maximize the weighted sum rate under perfect CSIs.Next, considering the imperfect CSIs from the IRS to users, we have redesigned a robust joint optimization algorithm. From simulation results, we have found that the channel estimation error has a large impact on the system sum rate. Moreover, allocating a higher weight to a particular user can improve that user's rate, but at the cost of sum rate. Consequently, channel estimation schemes and users weight selection are important criteria for the design of practical systems, and we need to adjust the weights according to different quality of service requirements of the users.

1. REFERENCES

2. Z. Piao, M. Peng, Y. Liu, and M. Daneshmand, "Recent advances of edge cache in radio access networks for internet of things: Techniques, performances, and challenges," IEEE Internet Things J., vol. 6, no. 1, pp. 1010–1028, Feb. 2019.
3. G. Yu, X. Chen, C. Zhong, D. W. Kwan Ng, and Z. Zhang, "Design, analysis, and optimization of a large intelligent reflecting surface-aided B5G cellular internet of things," IEEE Internet Things J., vol. 7, no. 9, pp. 8902–8916, Sep. 2020.
4. H. Sarieddeen, M. Alouini, and T. Y. Al-Naffouri, "Terahertz-band ultramassive spatial modulation MIMO," IEEE J. Sel. Areas Commun., vol. 37, no. 9, pp. 2040–2052, Sep. 2019.
5. R. Zhang, W. Hao, G. Sun, and S. Yang, "Hybrid precoding design for wideband THz massive MIMO-OFDM systems with beam squint," IEEE Sys. J., pp. 1–4, to be published, 2020.
6. S. Priebe and T. Kurner, "Stochastic modeling of THz indoor radio channels," IEEE Trans. Wireless Commun., vol. 12, no. 9, pp. 4445–4455, Sep. 2013.
7. L. Lu, G. Y. Li, A. L. Swindlehurst, A. Ashikhmin, and R. Zhang, "An overview of massive mimo: Benefits and challenges," IEEE J. Sel. Topics Signal Proc., vol. 8, no. 5, pp. 742–758, May 2014.
8. M. Zeng, X. Li, G. Li, W. Hao, and O. A. Dobre, "Sum rate maximization for IRS-assisted uplink NOMA," IEEE Commun. Lett., vol. 25, no. 1, pp. 234–238, Jan. 2021.
9. J. Zhang, E. Bjornson, M. Matthaiou, D. W. K. Ng, H. Yang, and D. J. ¨ Love, "Prospective multiple antenna technologies for beyond 5G," IEEE J. Sel. Areas Commun., vol. 38, no. 8, pp. 1637–1660, Aug. 2020.
10. Q. Wu and R. Zhang, "Intelligent reflecting surface enhanced wireless network via joint active and passive beamforming," IEEE Trans. Wireless Commun., vol. 18, no. 11, pp. 5394–5409, Nov. 2019.
11. Z. Chu, W. Hao, P. Xiao, and J. Shi, "Intelligent reflecting surface aided multi- antenna secure transmission," IEEE Wireless Commun. Lett., vol. 9, no. 1, pp. 108–112, Jan. 2020.
12. Y. Chen, Y. Wang, J. Zhang, and Z. Li, "Resource allocation for intelligent reflecting surface aided vehicular communications," IEEE Trans. Veh. Tech., vol. 69, no.10, pp. 12 321–12 326, Oct. 2020.
13. W. Hao, G. Sun, J. Zhang, P. Xiao, and L. Hanzo, "Secure millimeter wave cloud radio access networks relying on microwave multicast fronthaul," IEEE Trans. Commun.,

vol. 68, no. 5, pp. 3079–3095, May 2020.
14. C. Lin and G. Y. Li, "Adaptive beamforming with resource allocation for distance-aware multi-user indoor terahertz communications," IEEE Trans. Wireless Commun., vol. 63, no. 8, pp. 2985–2995, Aug. 2015.
15. ——, "Energy-efficient design of indoor mmwave and sub-THz systems with antenna arrays," IEEE Trans. Wireless Commun., vol. 15, no. 7, pp. 4660–4672, Jul. 2016.
16. S. A. Busari, K. M. S. Huq, S. Mumtaz, J. Rodriguez, Y. Fang, D. C. Sicker, S. Al-Rubaye, and A. Tsourdos, "Generalized hybrid beamforming for vehicular connectivity using THz massive MIMO," IEEE Trans. Veh. Tech., vol. 68, no. 9, pp. 8372–8383, Sep.2019.
17. J. Tan and L. Dai, "Delay-phase precoding for THz massive MIMO with beam split," in Proc. IEEE GLOBECOM, 2019, pp. 1–6.
18. H. Yuan, N. Yang, K. Yang, C. Han, and J. An, "Hybrid beamforming for terahertz MIMO-OFDM systems over frequency selective fading," arXiv e-prints, p. arXiv:1910.05967, 2019.
19. B. Ning, Z. Chen, W. Chen, Y. Du, and J. Fang, "Terahertz multi-user massive MIMO with intelligent reflecting surface: Beam training and hybrid beamforming," IEEE Trans. Veh. Technol., to be published, 2021.
20. S. Zhang and R. Zhang, "Capacity characterization for intelligent reflecting surface aided MIMO communication," IEEE J. Sel. Areas Commun., vol. 38, no. 8, pp. 1823–1838, Aug. 2020.
21. Y. Yang, B. Zheng, S. Zhang, and R. Zhang, "Intelligent reflecting surface meets OFDM: Protocol design and rate maximization," IEEE Trans. Commun., vol. 68, no. 7, pp. 4522–4535, Jul. 2020.